Structural insights into VLDLR recognition by Western Equine Encephalitis Virus

Shengjian Liang, et. al.

Supplementary information：

Supplementary Figures 1-11

Supplementary Tables 1-2

Supplementary Figure 1

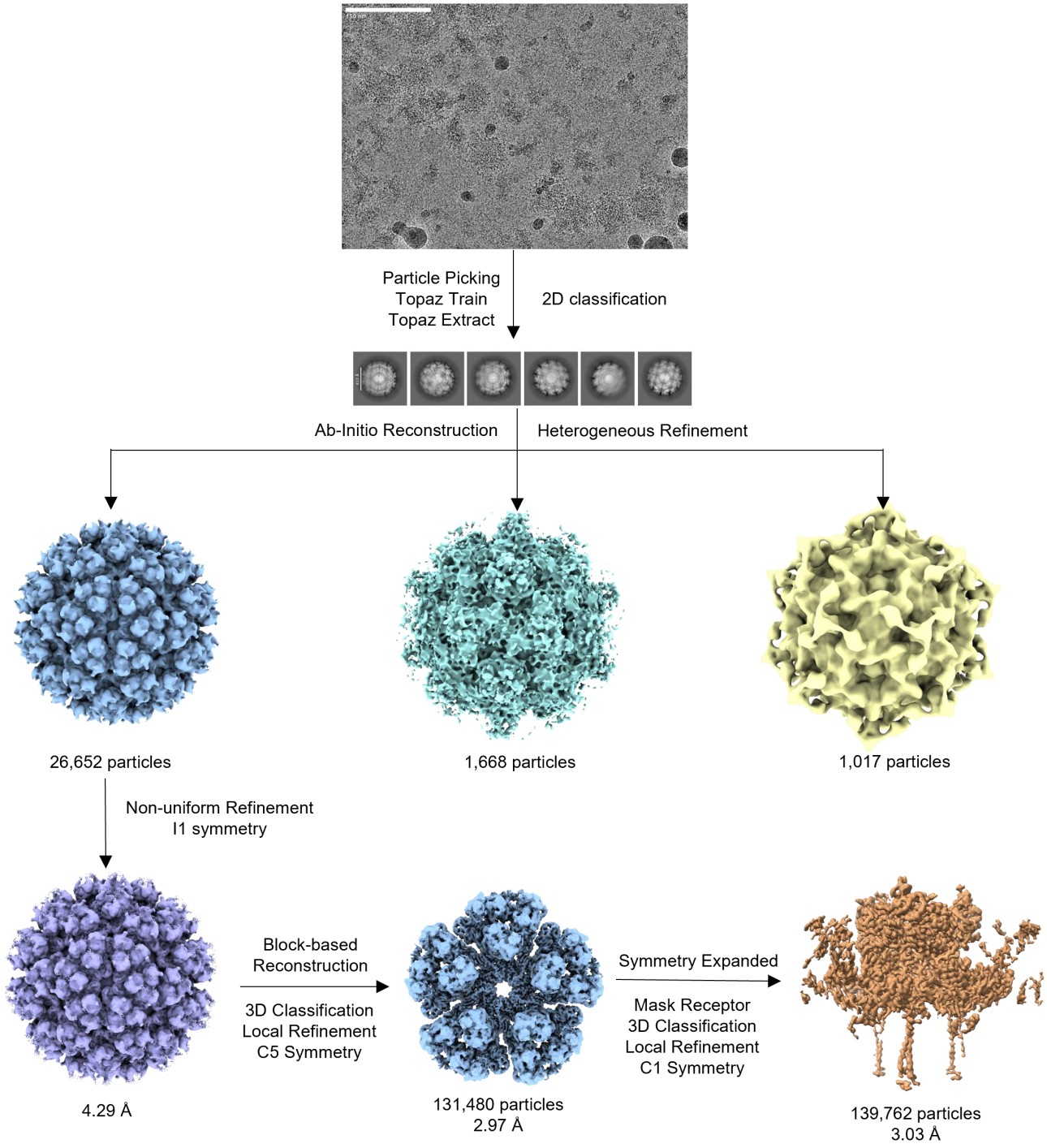

Supplementary Figure 1. Cryo-EM reconstruction workflow of WEEV VLPs in complex with VLDLR-LA1-3.

Supplementary Figure 2

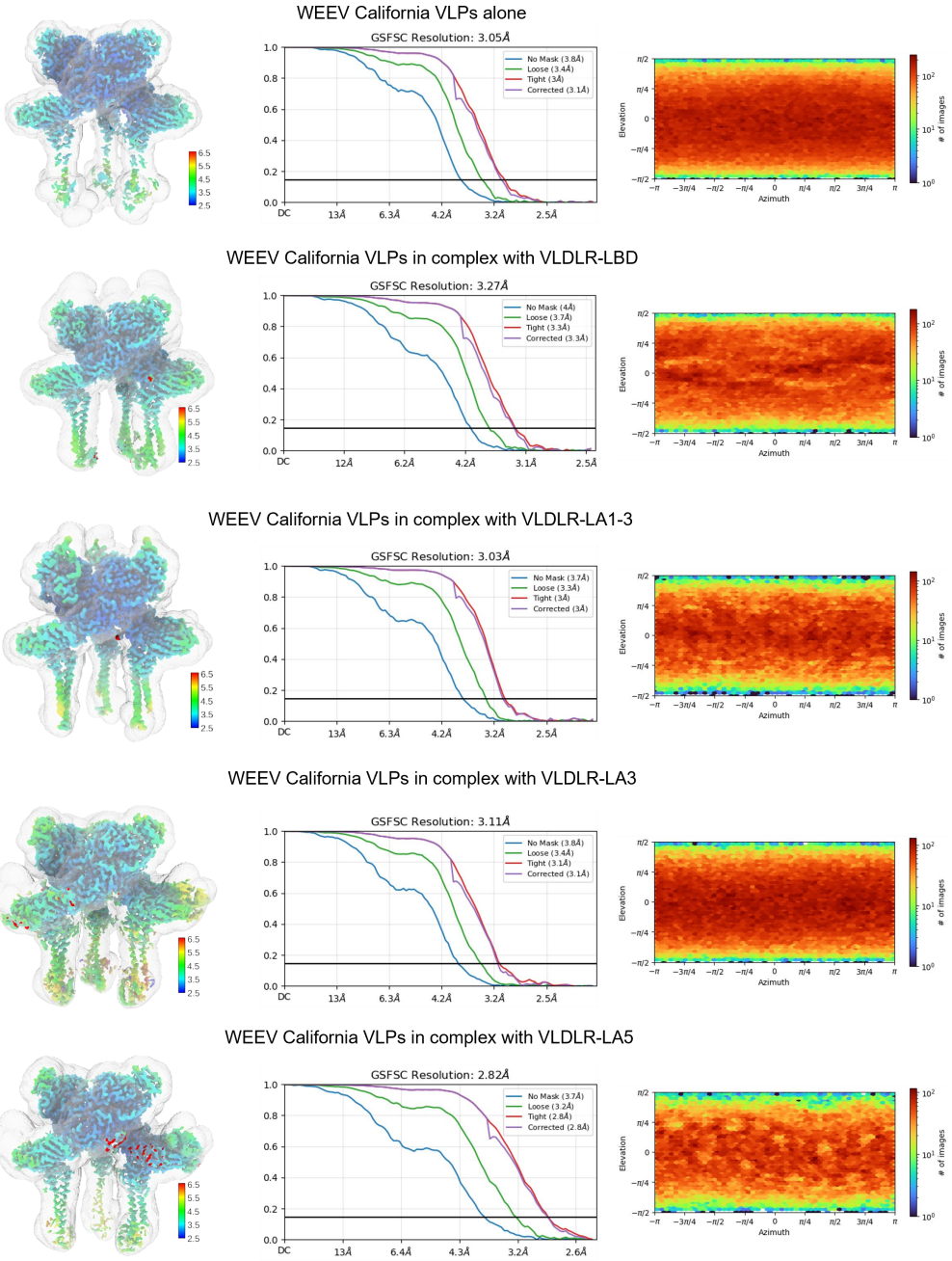

Supplementary Figure 2. Cryo-EM quality estimate, related to Figures 1 and 3. The local resolutions (left) were estimated in cryoSPARC and are indicated by the bars and Fourier shell correlation (FSC) (middle) of the 3D reconstructions for VLPs or the q3 spike following gold standard refinement. FSC curves are plotted after masking. Angular distribution calculated in cryoSPARC (right).

Supplementary Figure 3

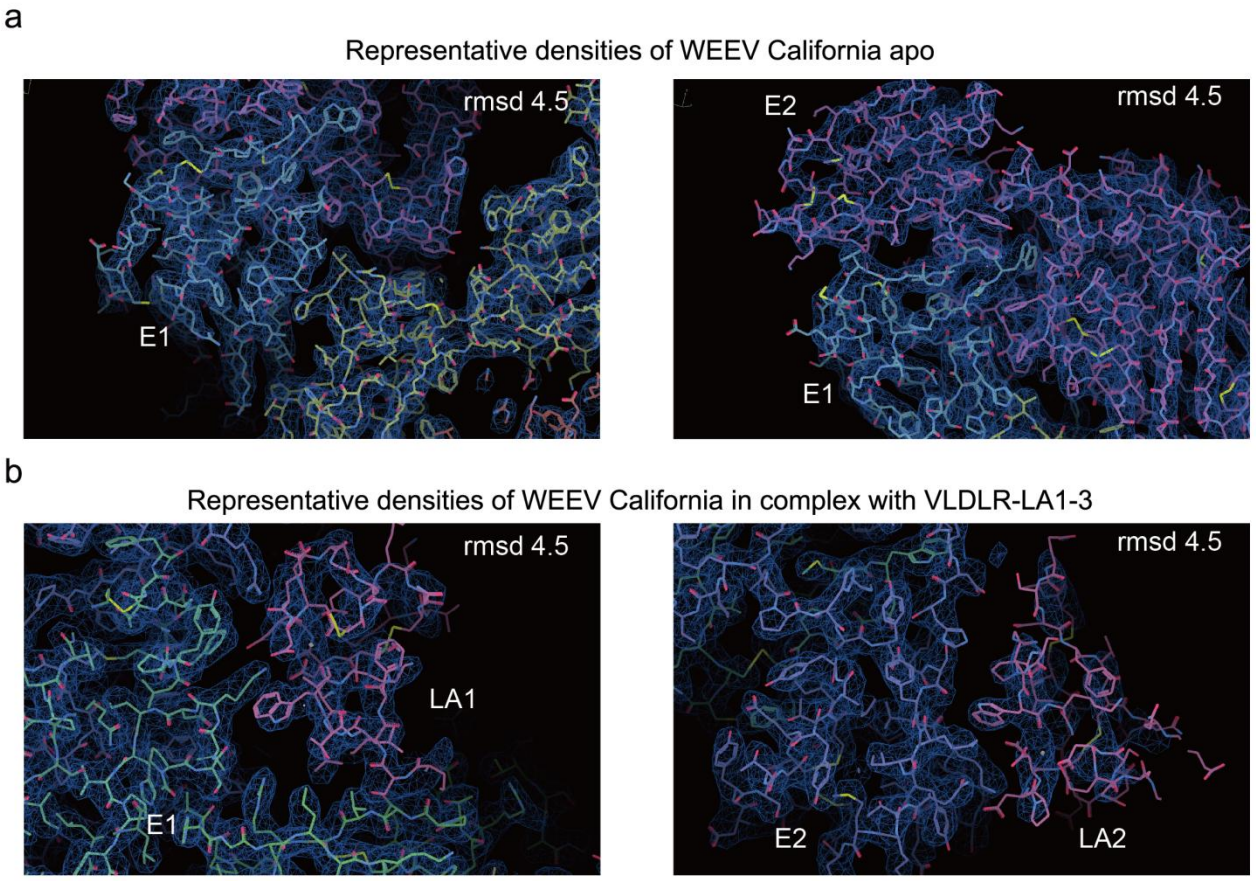

Supplementary Figure 3. Representative densities. (a) Representative densities of WEEV California apo. **(b)** Representative densities of WEEV California in complex with VLDLR-LA1-3.

Supplementary Figure 4

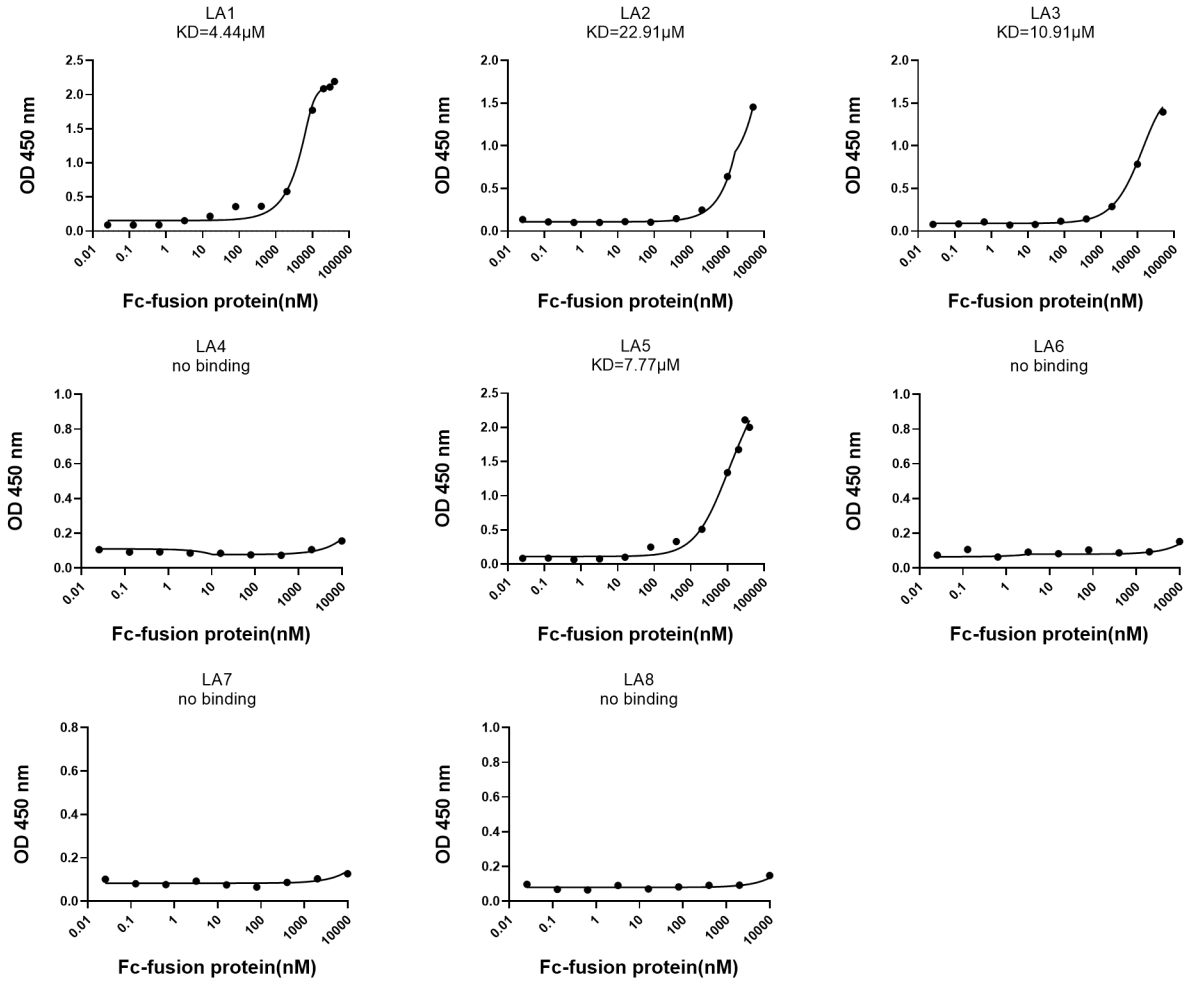

Supplementary Figure 4. ELISA analysis of different LA repeats. Binding of different LA repeats-Fc fusions to WEEV VLPs measured by enzyme-linked immunosorbent assay (ELISA). The equilibrium dissociation constant (K_D) was calculated as mean of two biologically independent experiments.

Supplementary Figure 5

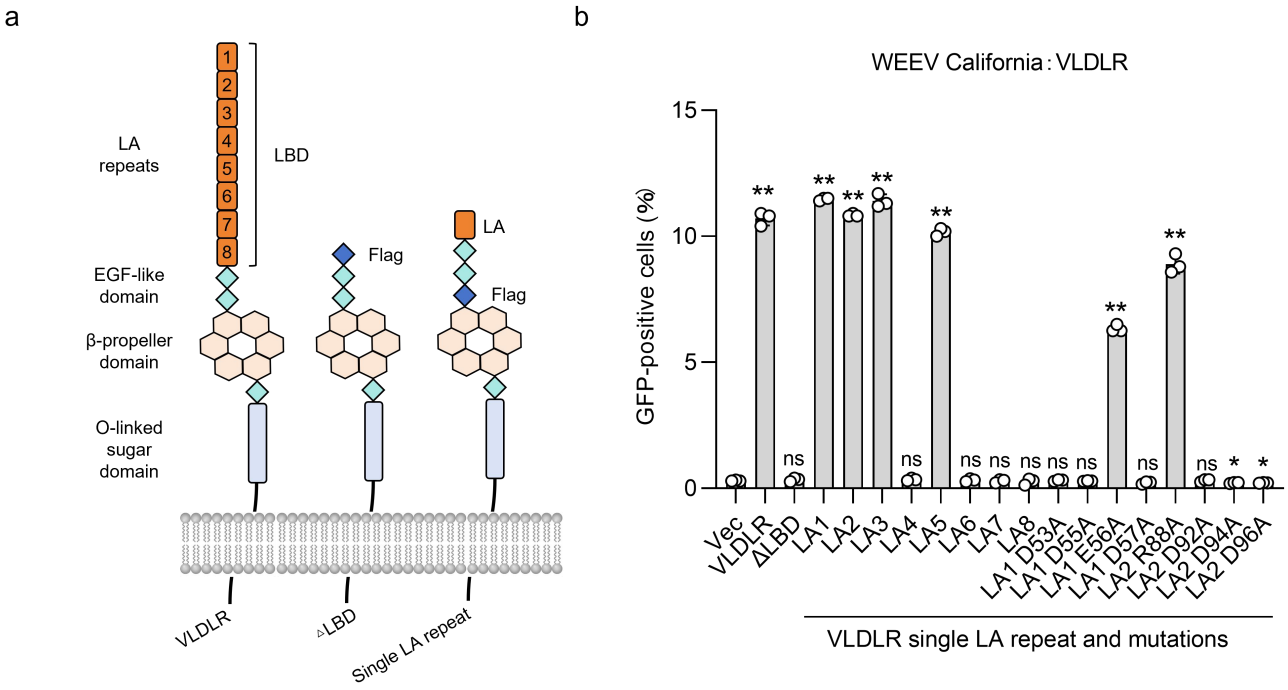

Supplementary Figure 5. Cell-based assays for the impacts of VLDLR single LA repeat and mutants on WEEV infection. (a) Schematic diagram of a single LA repeat. **(b)** K562 cells stably expressing indicated VLDLR proteins were infected with VSV-WEEV (California) (MOI = 0.2) for 24 h. Infection was monitored by flow cytometry . Expression of the indicated proteins was confirmed by immunoblots. Data are mean ± SD from 3 biological repeats (n=3) and p values are from unpaired two-tailed Student's t-test. At least three independent experiments were performed with similar results and representative images are shown. All t-test data for the experimental groups were calculated relative to the Vec as the control. Source data are available as a Source Data file.

Supplementary Figure 6

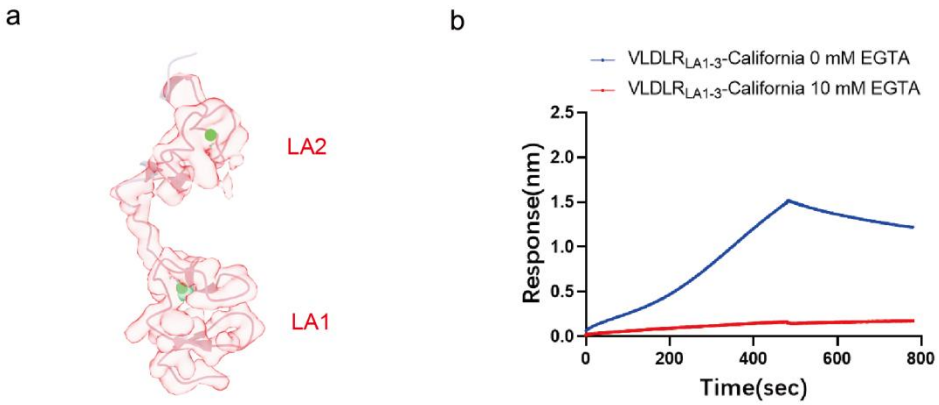

Supplementary Figure 6. The effect of calcium ions on the binding of WEEV VLPs to VLDLR-LA1-3. (a) The structure of VLDLR-LA1-3 is fitted into the cryo-EM density of the WEEV California VLP-VLDLR-LA1-3 complex. The density corresponding to two calcium ions is colored green. The density corresponding to LA1 and LA2 is colored red. **(b)** The binding and dissociation curves of WT VLDLR-LA1-3 with WEEV California VLPs with 0, 10 mM EGTA are shown.

Supplementary Figure 7

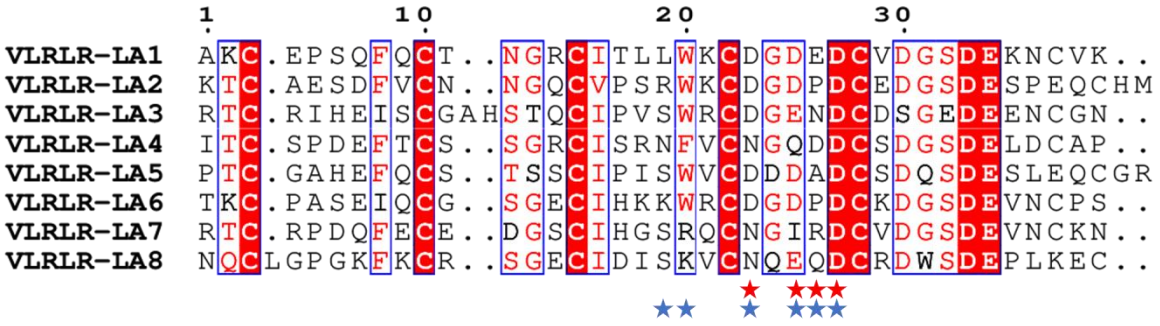

Supplementary Figure 7. Sequence alignment of eight LA repeats. The sequences' eight LA repeats were aligned in Clustal Omega and were colored using ESPript 3.0. The key interacting residues in LA1 and LA2 are indicated with red stars and blue stars, respectively.

Supplementary Figure 8

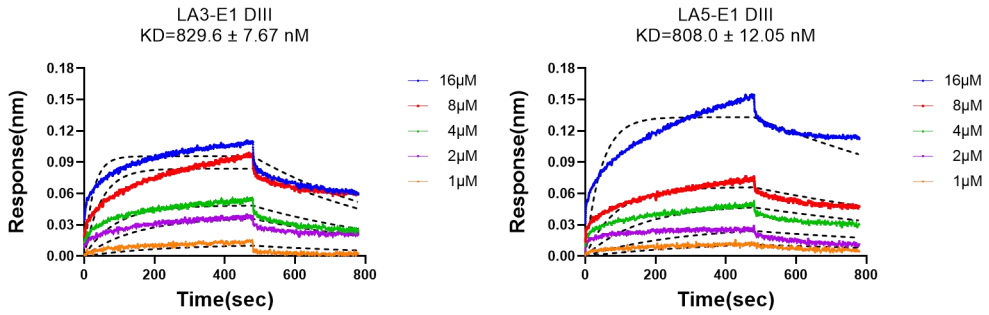

Supplementary Figure 8. BLI analysis of VLDLR LA3 and LA5 with WEEV California E1-DIII Biolayer interferometry binding analysis of VLDLR LA3 (left panel) and LA5 (right panel) to WEEV California E1-DIII. The displayed results were obtained from a single technical replicate and are representative of three biologically independent experiments. The equilibrium dissociation constant (K_D) was calculated as the mean ± standard deviation (SD; n = 3).

Supplementary Figure 9

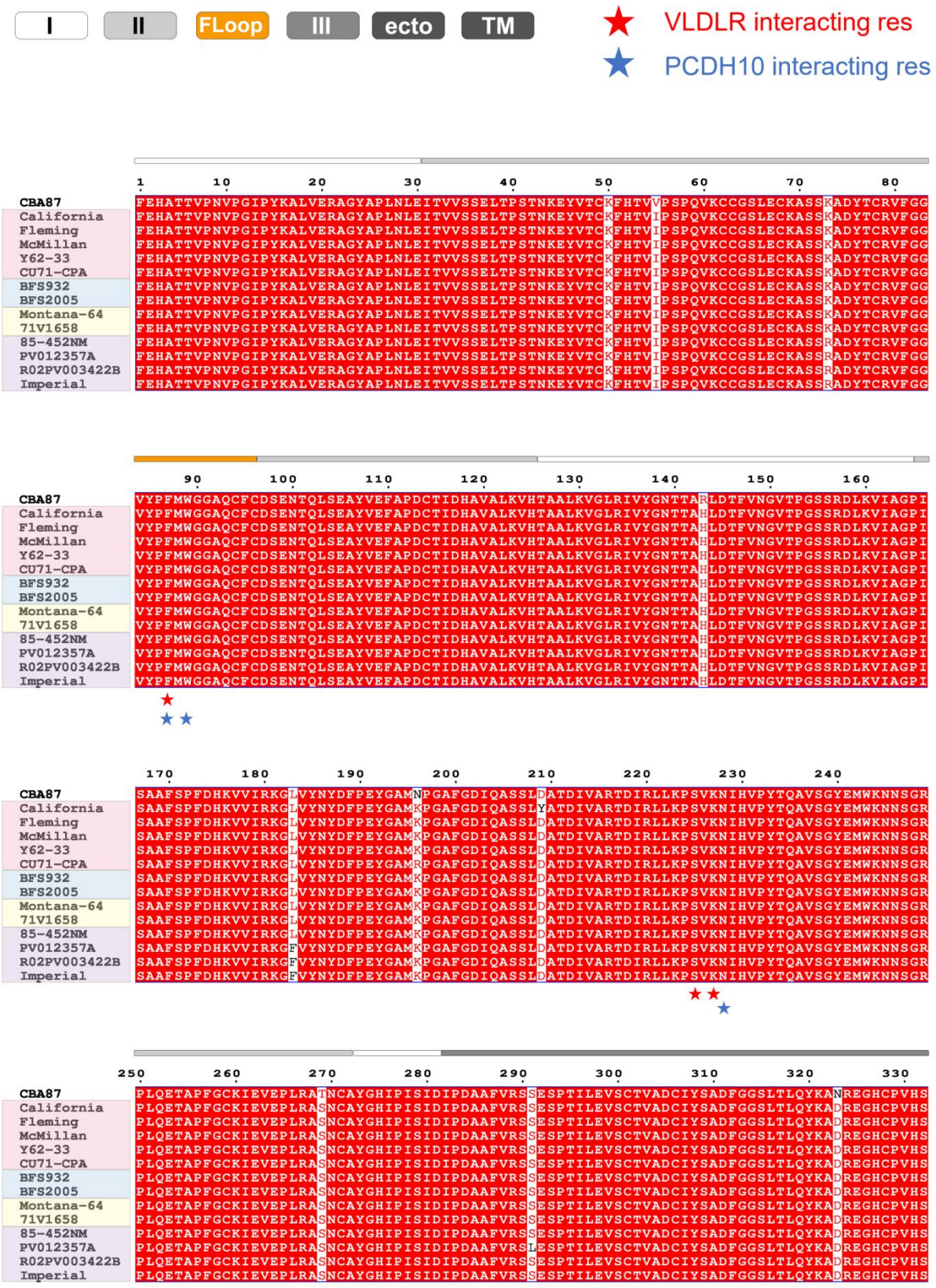

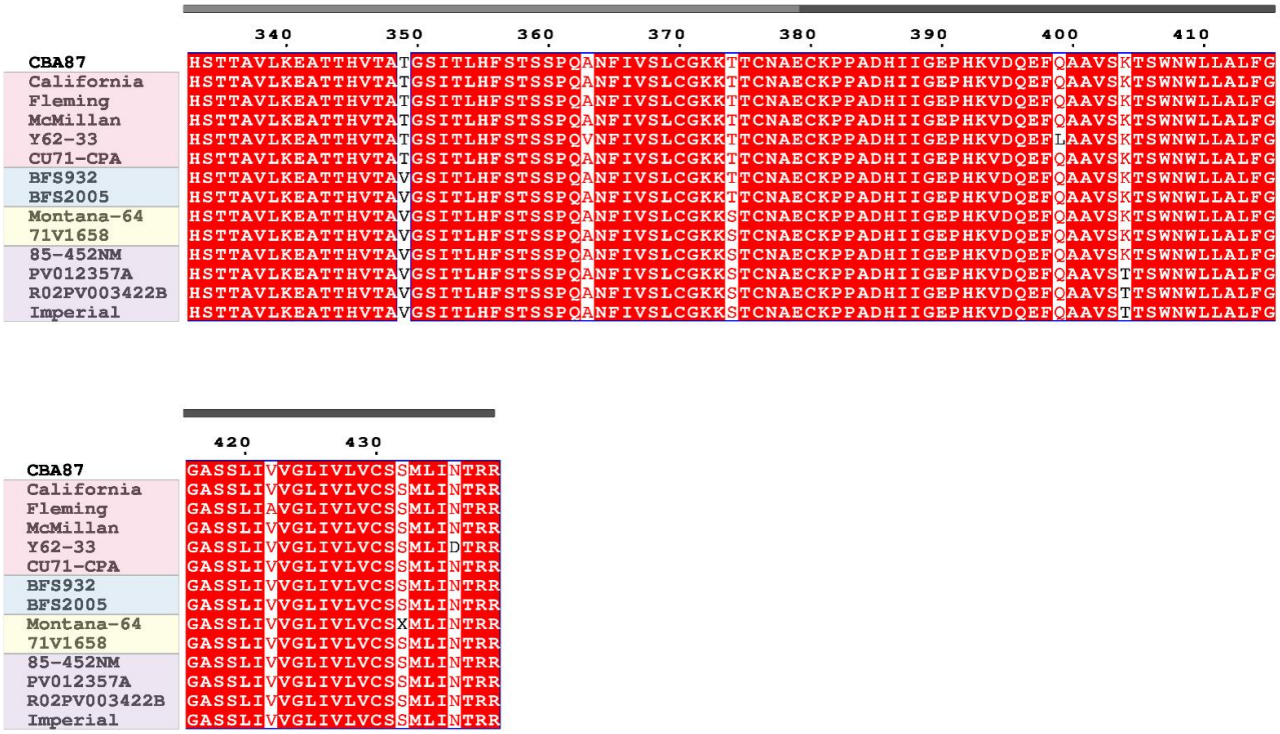

Supplementary Figure 9. Sequence alignment of E1 proteins of the WEEV strains. The WEEV strains for comparison include CBA87 in group C; California (1930), Fleming (1938), McMillan (1941), Y62-33 and CU71-CPA in group A; BFS2005 (1954) and BFS932 (1946) in group B1; Montana-64 (1967) and 71V1658 (1971) in group B2; 85-452NM (1985) and PV012357A (2001), as well as R02V003422B (2005) and Imperial 181 (2005), in group B3. Sequences were aligned by Clustal Omega and were colored using ESPript 3.0. Red boxes indicate residues that are strictly conserved; white boxes and red letters indicate conserved residues within the specific group; white boxes and black letters indicate non-conserved residues. Domains of E1 protein are indicated by colored bars above the sequence alignment: A (white), B (light gray), C (medium gray), ectodomain and TM (deep gray), and fusion loop (orange). Interacting residues with VLDLR and PCDH10 (distance less than 4.0 Å) are indicated by red and blue stars.

Supplementary Figure 10

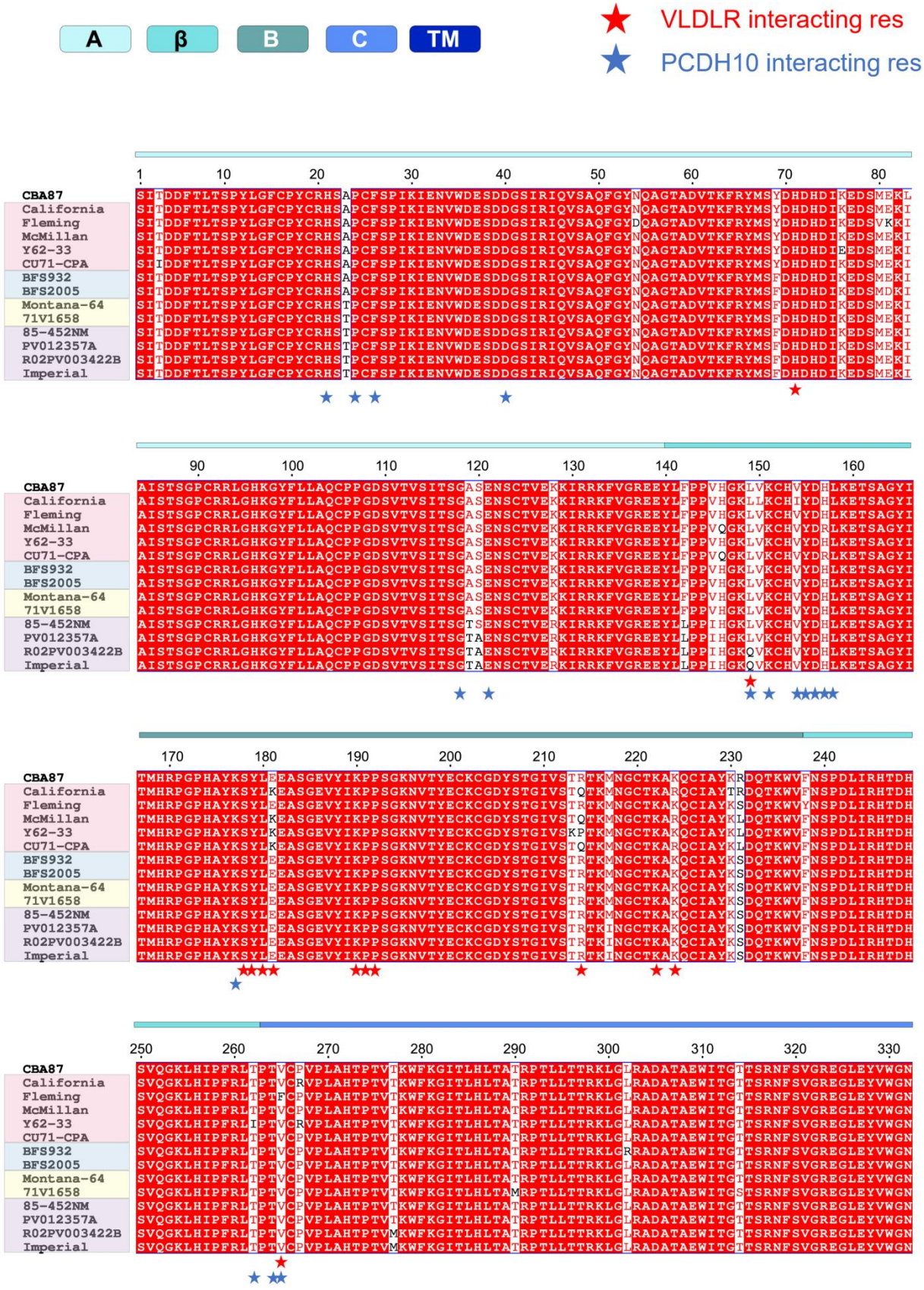

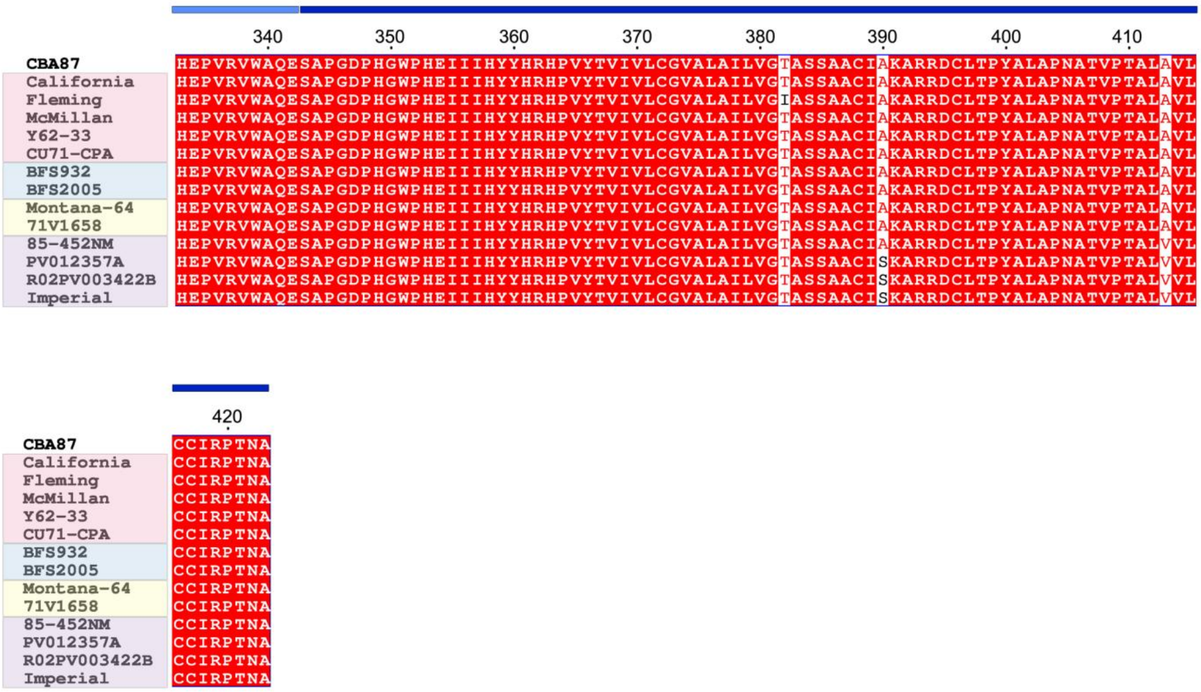

Supplementary Figure 10. Sequence alignment of E2 proteins of the WEEV strains. The sequences of E2 proteins encoded by various WEEV strains were aligned and shown. Domains of E2 protein are indicated by colored bars above the sequence alignment: A (pale cyan), beta (light teal), B (deep teal), C (sky blue), and TM (deep blue). Interacting residues with VLDLR and PCDH10 (distance less than 4.0 Å) are indicated by red and blue stars.

Supplementary Figure 11

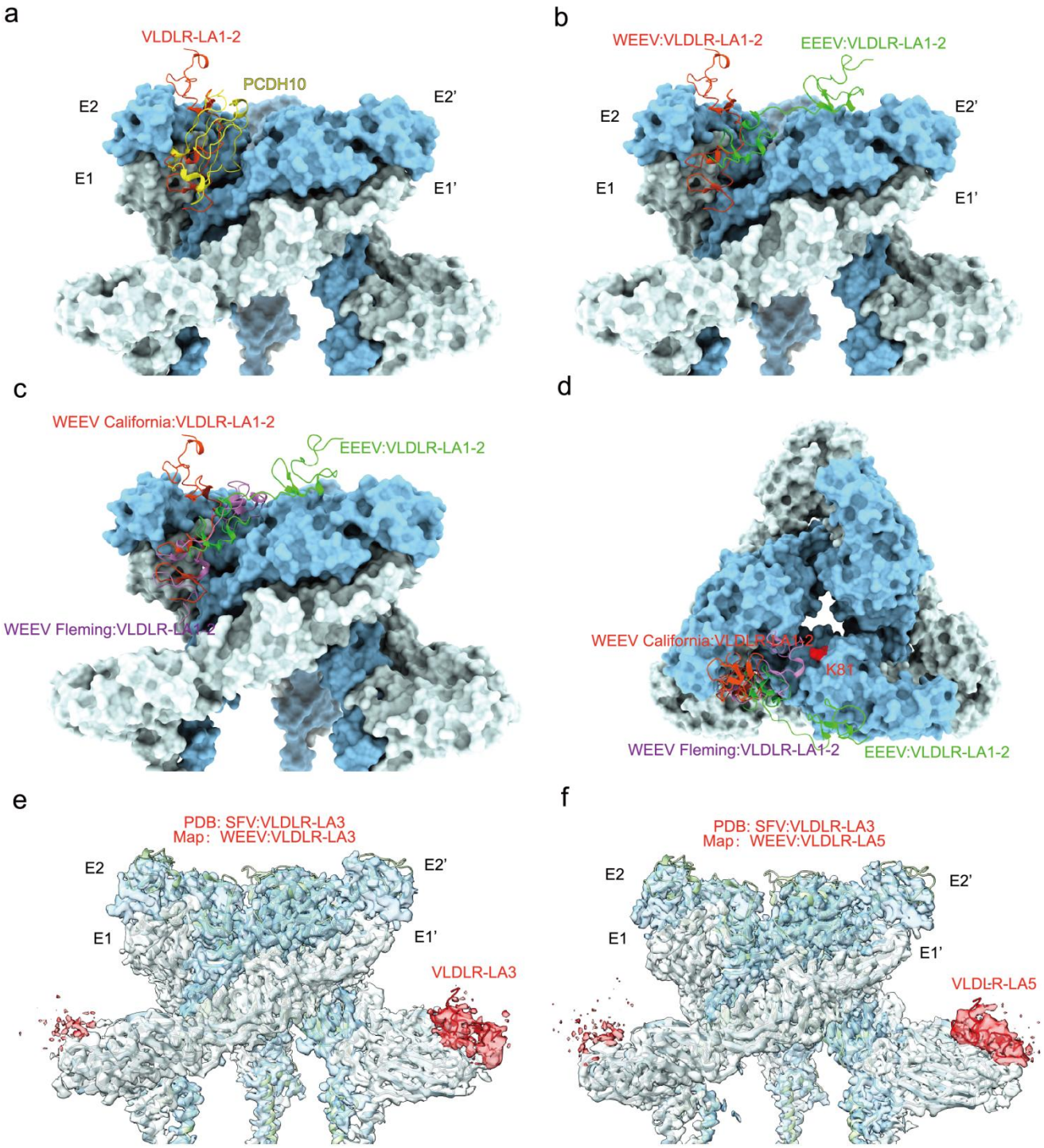

Supplementary Figure 11. Comparative receptor recognition by WEEV, EEEV, and SFV. **(a)** Comparison of WEEV binding to VLDLR and PCDH10 (PDB: 9L41). The E1E2 proteins of WEEV were aligned using Coot to illustrate the binding modes. **(b-d)** Depiction of the interactions of VLDLR with WEEV California, EEEV (PDB: 8XI4), WEEV Fleming (PDB: 9E9Z),

and SFV (PDB: 8IHP). The E1E2 proteins of WEEV California and EEEV (PDB: 8XI4) were aligned in Coot to highlight the differences in VLDLR recognition (b). The E1E2 proteins of WEEV California, WEEV Fleming (PDB: 9E9Z), and EEEV (PDB: 8XI4) were aligned in Coot to highlight the differences in VLDLR recognition (c). (d) The top view of figure (c), The PDB structure of SFV:VLDLR-LA3 (PDB: 8IHP)was fitted into the cryo-EM density map of WEEV:VLDLR-LA3 (c) and WEEV:VLDLR-LA5 (d).

Supplementary Table 1. Cryo-EM data collection, processing, and structure determination

	WEEV California VLP	WEEV California VLP:VLDLR-LA1-3	WEEV California VLP:VLDLR-LBD	WEEV California VLP:VLDLR-LA3	WEEV California VLP:VLDLR-LA5
PDB entry	9UIH	9UIO	9WSL		
EMBD entry for local refinement	EMD-64194	EMD-64199	EMD-66198	EMD-64263	EMD-64264
Data collection and processing					
Magnification	81,000	81,000	105,000	81,000	105,000
Voltage (kV)	300	300	300	300	300
Electron exposure (e^{-}/Å^2)	50	50	50	50	50
Defocus range (μm)	-1.0 to -2.0	-1.0 to -2.0	-1.0 to -2.0	-1.0 to -2.0	-1.0 to -2.0
Pixel size (Å)	1.055	1.055	1.2	1.055	1.2
Symmetry imposed	I1	I1	I1	I1	I1
Initial particle images (no.)	30,162	39,285	247,657	16,449	22,942
Final particle images (no.)	14,411	25,959	19,830	13,367	19,777
Map resolution (Å)	6.12	4.29	5.09	5.02	4.78
FSC threshold	0.143	0.143	0.143	0.143	0.143
Refined blocks					
Symmetry imposed	C1	C1	C1	C1	C1
Final particle images (no.)	292,435	139,762	176,404	169,438	106,612
Map resolution (Å)	3.05	3.03	3.27	3.11	2.82
Refinement					
Model resolution (Å)	3.05	3.03	3.27	3.11	2.82
FSC threshold	0.143	0.143	0.143	0.143	0.143
Model resolution range (Å)	∞ to 3.05	∞ to 3.03	∞ to 3.27	∞ to 3.11	∞ to 2.82
Map sharpening *B* factor (Å^2)	98.3	87.6	106.4	82.8	65.2
Model composition					
Non-hydrogen atoms	19,782	21,591	21,591		
Protein residues	2571	2,808	2,808		
Ligands	0	6	6		
B factors (Å^2)					
Protein	154.39	256.68	344.94		
Ligand	N/A	136.22	318.19		
R.m.s. deviations					
Bond lengths (Å)	0.003	0.003	0.004		
Bond angles (°)	0.667	0.595	0.610		
Ramachandran plot					
Favored (%)	94.61	94.98	94.84		

Allowed (%)	5.39	5.02	5.09
Disallowed (%)	0.00	0.00	0.07
clash score	6.95	7.51	7.70
rotamer outliers (%)	2.93	2.42	2.92
Cβ outliers (%)	NA	NA	NA
CC (mask)	0.89	0.90	0.86

Supplementary Table 2. Summary of the BLI measured binding affinities.

VLDLR single LA repeat	K_D (nM)		k_{on} (10^5/Ms)		k_{dis} (10^{-5}/s)	
LA1	0.122 0.091 0.126	0.11 ± 0.001	66.4 97.4 49.4	71.1 ± 0.36	80.9 88.4 62.2	77.2 ± 0.63
LA2	1.749 1.659 1.350	1.59 ± 0.025	9.5 11.3 5.7	8.8 ± 0.12	166.1 187.7 77.1	143.6 ± 0.58
LA3	3.101 7.166 7.990	6.09 ± 0.449	3.9 2.3 0.8	2.3 ± 0.08	121.0 163.3 60.1	114.8 ± 0.52
LA4	ND ND ND	ND	ND ND ND	ND	ND ND ND	ND
LA5	0.236 0.622 0.253	0.37 ± 0.003	41.4 16.9 48.1	35.5 ± 0.21	97.8 104.7 122.0	108.2 ± 0.68
LA6	ND ND ND	ND	ND ND ND	ND	ND ND ND	ND
LA7	ND ND ND	ND	ND ND ND	ND	ND ND ND	ND
LA8	ND ND ND	ND	ND ND ND	ND	ND ND ND	ND